Differential Radiometers Using Fabry-Perot Interferometric Technique for Remote Sensing of Greenhouse Gases

Elena M. Georgieva, William S. Heaps, Emily L. Wilson

Abstract— A new type of remote sensing radiometer based upon the Fabry-Perot interferometric technique has been developed at NASA's Goddard Space Flight Center and tested from both ground and aircraft platforms. The sensor uses direct or reflected sunlight and has channels for measuring column concentration of carbon dioxide at 1570 nm, oxygen lines sensitive to pressure and temperature at 762 and 768 nm, and water vapor (940 nm). A solid Fabry-Perot etalon is used as a tunable narrow bandpass filter to restrict the measurement to the gas of interest's absorption bands. By adjusting the temperature of the etalon, which changes the index of refraction of its material, the transmission fringes can be brought into nearly exact correspondence with absorption lines of the particular species. With this alignment between absorption lines and fringes, changes in the amount of a species in the atmosphere strongly affect the amount of light transmitted by the etalon and can be related to gas concentration. The technique is applicable to different chemical species. We have performed simulations and instrument design studies for CH_4, $^{13}CO_2$ isotope, and CO detection.

***Index Terms*— Absorbing media, Atmospheric measurements, Fabry-Perot interferometers, Optical interferometry, Remote sensing.**

I. Introduction

Precise detection of carbon dioxide in the atmosphere is of great interest due to its impact on trapping the long wavelength radiation emitted from the Earth's surface. There are different scenarios about the detailed causes for the global warming of the Earth's atmosphere. The net impact of anthropogenic aerosol emissions and greenhouse gases is a complex study [1]. Recent climate models focus more on the effects of aerosol, which can absorb solar energy and warm the atmosphere. However the indirect effects also occur when aerosol change the cloud optical properties and reflect the solar energy back into space [2,3,4,5]. Studies have shown that aerosol and greenhouse gas forcing are almost of the same order of magnitude [1,3]. However while the anthropogenic aerosols have short lifetime, the carbon dioxide is a long-lived constituent. The concentrations of the principal anthropogenic greenhouse gases (CO_2, CH_4, N_2O) have increased substantially during the industrial period. The carbon dioxide concentration has increased by more than 95 ppmv in the last 150 years due to the emissions of the modern industrial revolution and the mixing ratio has become 380 ppmv [6, 7]. In this same time frame, the concentration of atmospheric methane has increased by 150 percent from approximately 700 to 1,745 ppbv [8, 9]. Although found in lower concentrations than carbon dioxide, methane is about 20 times more effective in absorbing infrared radiation. While the majority of CO_2 variability occurs in the lower atmosphere (~1000 to 800 mbar), satellite instruments measure the total atmospheric column. Since sources and sinks at the surface represent a small perturbation to the total column, a precision of better than 1% is required [10, 11]. That number comes from the transport inversion model experiments, which indicate that global column measurements with a precision better than 1% (3ppmv on the 380 ppmv background) on a time scale of one month is the science requirement to improve surface flux estimates beyond the capability of the existing network [11]. The natural geographic distribution and temporal variability of CO_2 sources and sinks are still not well understood, and more monitoring instruments are needed to quantify the carbon dioxide dynamics and to help predict climate change [12,13]. The water vapor concentration resulting from evaporation of water from land and ocean is enhanced by carbon dioxide. As carbon dioxide absorbs radiative heat from the Earth's surface - warming the atmosphere, atmospheric water vapor increases because the warmer air can hold more water [14]. The increased water vapor leads to an increase in the greenhouse effect and further increase in temperature; the cycle is repeated until equilibrium. For climate research, high precision (error<5%) water vapor measurements are needed with global coverage [15].

Our knowledge of atmospheric carbon processes comes from satellites (Atmospheric Infrared Sounder,

Manuscript received September 28, 2007. This work was supported in part by the NASA Earth Sun-System Technology Office (ESTO), Instrument Incubator Program (IIP), grant NRA-01-OES-01.

Elena Georgieva is with Goddard Earth Science and Technology Center, University of Maryland Baltimore County and NASA's Goddard Space Flight Center, Greenbelt, MD, 20771, USA

W. S. Heaps is with the Instrument Systems and Technology Division (ISTD) at NASA GSFC, Greenbelt, MD, 20771,

E. L Wilson is with the Laser & Electro-Optics Branch, NASA/GSFC

SCIAMACHY onboard ENVISAT satellite [16]) and ground network measurements. The latter consists of two main sources- the long term, in situ CO_2 measurement program led by the NOAA Climate Monitoring and Diagnostics Laboratory and the TransCom 3 transport/flux estimation experiment [17, 18]. These in situ measurements are very precise (uncertainties on the order of 0.1 ppm) and accurate, but are necessarily limited in time and space. Rayner and O'Brien [11] predicted that the required accuracy for monthly averaged CO_2 column data needs to be better than 2.5 ppmv on 8^0 x 10^0 footprint for comparable performance to a moderate surface network. Such a precision is difficult to achieve.

The instrument that we have developed and tested on two flight campaigns detects the absorption of CO_2, O_2 and H_2O gases using direct or reflected sunlight [19, 20, 21, 22, 23]. The sensor makes use of two features of the Fabry-Perot interferometer to achieve high sensitivity: high spectral resolution resulting from matching the width of an atmospheric absorption feature to the instrumental band pass, and high optical throughput enabled by simultaneous use of multiple spectral lines. For any species that one wishes to measure, this first feature is available while the use of multiple spectral features can be employed only for species with suitable spectra and freedom from interfering species in the same wavelength region. Throughput of an interferometer can be as much as two orders of magnitude larger than a spectrometer with a grating with the same resolution, which means larger signals or better signal-to-noise ratio (S/N). Our sensor records data every 0.1 s, has high spectral selectivity and has only one moving part (chopper), which makes it an ideal candidate for an airborne or satellite mission. It can work also as a ground based sensor using direct light from the Sun. The current goal is to develop a precise, inexpensive, ground based device sensitive enough to measure column averaged CO_2 and suitable for wide deployment as a validation instrument for the Orbiting Carbon Observatory (OCO) satellite [24, 25, 26, 27]. This will fill the gaps of the sparse ground network and help to understand the global distribution of CO_2 and its role in climate change. Parallel to that we are developing a new sensor for methane detection and working on simulations for systems to measure CO and $^{13}CO_2$ isotope.

II. DESCRIPTION OF INSTRUMENT AND BASIC THEORY

The incoming light is split into the three wavelength bands with a dichroic beam splitter and directed into CO_2, O_2 pressure-sensitive and O_2 temperature-sensitive channels. The optical schematic for the CO_2 channel of the FP instrument is shown in Fig.1. In this design, incoming light is focused onto a 2 mm diameter aperture to define the field of view. The light is modulated at ~400 Hz with a chopper and then re-collimated as it emerges from the aperture. The incident light in the CO_2 channel is pre-filtered at a central wavelength of 1570 nm. The light then splits between the Fabry-Perot and Reference sub-channels with 90% of the light going to the Fabry-Perot sub-channel. In the Fabry-Perot sub-channel the light passes through the Fabry-Perot etalon mounted in a temperature controlled oven for fine FSR (free spectral range) tuning. By adjusting the temperature of the etalon, which changes the index of refraction of its material, the transmission fringes can be brought into nearly exact correspondence with absorption lines of the particular species (Fig.2). A set of off axis parabolic (OAP) gold mirrors focuses light onto InGaAs detectors for the CO_2 sub-channels and Si detectors for the two oxygen channels. For bringing light into the instrument we use fiber bundles, which intentionally scramble the incident light to remove spatial information. The Fabry-Perot etalons in this instrument are solid fused silica etalons and they have different thickness for each instrument channel. For the CO_2 channel the etalon has a free spectral range (FSR) of 0.306 nm, a refractive index of 1.443 at λ=1571 nm, and a clear aperture of 50 mm with highly reflective coatings on both surfaces. The light that passes through the etalon undergoes multiple reflections on each inside surface, creating an interference pattern of equidistant fringes as a function of frequency. The width of the pass bands depends on the coatings quality and on the flatness and parallelism of the surfaces. The Fresnel formalism gives the reflected and transmitted amplitude components for the light wave as functions of the optical constants of the two media and the angle of incidence. The resulting intensity follows the Airy function distribution pattern. The ideal Fabry-Perot etalon with perfectly flat surfaces transmits a narrow spectral band and the energy transmission coefficient I_T is given by [28, 29]:

$$I_T = \frac{T^2}{(1-R)^2}\left[1+\frac{4R}{(1-R)^2}\sin^2\left(\frac{2\pi n d\cos\theta}{\lambda}\right)\right]^{-1} \quad (1)$$

where λ is the wavelength, n is the refractive index, d is the thickness of the etalon and θ is the angle of incidence within the cavity, T is the intensity transmission coefficient for each coating and R is the intensity reflection coefficient. The transmission is periodic.

III. EXPERIMENTAL

A. Data taken with the flight version of the FP radiometer

Carbon dioxide and oxygen column measurements using FP radiometer have been demonstrated in laboratory, ground based and airborne experiments. Water vapor channel was added recently and has been tested in the lab and ground based measurements. The FP radiometer is taking daily measurements at Goddard as a ground based sensor and the CO_2, O_2 and H_2O columns are measured

through absorption of light by those species in the atmosphere directly between the sun and the instrument. We accomplished this by collecting light with a small telescope fixed to an equatorial mount, aligned to track the sun throughout the day. An optical fiber coupled at the rear of the collimator brings light into the instrument. The initial tests indicate that the instrument can detect changes in the CO_2 column as small as 2.3 ppm with a one second average and better than 1 ppm in less than 10 seconds of averaging. The precision of the oxygen column pressure changes is as small as 0.88 mbar. Water vapor precision is 2 percent for one second of averaging. Figure 3 illustrates a typical data set collected over the course of a clear day with the instrument. The ratio of Fabry-Perot to reference signals is inversely proportional to absorption for CO_2 and H_2O and directly proportional for O_2 which is plotted on an inverted scale. Figure 4 shows the same data plotted as a function of the calculated air mass (the pathlength of the sunlight through the atmosphere between the sun and the instrument). The air mass decreases all morning until local noon and then increases until sunset. The air mass m is expressed by the Chapman function in the IDL program (Interactive Data Language) for data analysis so we can account for the sphericity of the Earth.

$$m_i = \frac{1}{\tau_i}\int_{z_0}^{\infty}\sigma_i(z)\frac{dz}{\left[1-\left(\frac{n_0 z_0}{nz}\sin\theta_0\right)^2\right]^{1/2}} \qquad (2)$$

where m is the air mass, τ is the optical depth, σ is the extinction coefficient as a function of altitude z, θ is the zenith angle of the sun, n is the atmospheric index of refraction. For very small solar zenith angles the air mass is equal to the secant of the zenith angle and that is the plane-parallel approximation.

The O_2 data essentially lie on top of one another because the atmospheric pressure (and hence the O_2 column) was constant on this day. The CO_2 channel shown in blue has some slight variability. CO_2 is expected to change very slightly on a diurnal basis because of the consumption of CO_2 by plants during the day. CO_2 has also a seasonal variability with maxima in spring and minima in the late summer [30].Those variations reflect changes in the biological sinks and can range from 1 ppmv in the Southern hemisphere (SH) to more than 20 ppmv in the Northern hemisphere (NH).

The variation in the water vapor column is shown to be real in a comparison with total column measurements by NOAA using GPS (Global Positioning System) technology. This result verifies that instruments of this type function properly and can be calibrated precisely. Figure 5 shows this inter-comparison of H_2O measurement by the Fabry-Perot instrument system and by a NOAA GPS based sensor located in Annapolis, Maryland for 5 days in late June and early July. The FP radiometer only operates during the day. Agreement is consistent with variability expected for sites ~30 miles apart.

For the airborne or satellite measurements the light passing through the atmosphere reflects on the Earth's surface before entering the instrument platform. The flight hardened version of the instrument was tested at two flight campaigns at NASA Dryden Research Center and at New Hampshire for the Polar Aura Validation campaign on NASA's DC-8 research airplane. Flights were conducted over a variety of surfaces (vegetation, water, snow) and under different atmospheric conditions. An in situ instrument provided CO_2 profiles up to the flight altitude. Temperature and density profiles were available from the aircraft data system. Comparison of FP radiometer data at different altitudes with the integrated in situ profiles formed the basic measure of the remote sensing sensitivity and provided a reference calibration. Data for the airborne tests were collected viewing in nadir direction. Simultaneous measurements of carbon dioxide and oxygen are shown in Figure 6(a,b). In both plots, the ratio of Fabry-Perot to Reference signals are compared to the altitude of the plane, corresponding to changes in the total path length of sunlight through the absorber. For CO_2 channel the ratio of Fabry-Perot to Reference signals (blue) are inversely proportional to the column of CO_2 measured and consequently the altitude from which measurements are made (red). As expected, changes in ratio clearly track changes in altitude. We have used the change in ratio with altitude to estimate the instrument response. We obtained a value of -0.44 for the change in ratio divided by the change in total column - indicating a ratio change of approximately 40% for a change of one air mass. Improvements to the instrument since this time have increased this value. Results from the flight experiments were reported [19, 20, 22]. The airborne instrument using light reflected off the ground has a 2% precision. The precision for the airborne experiments is reduced because the aerosol and cirrus scattering significantly alter the sunlight path through the atmosphere and hence the spectral attenuation. Atmospheric scattering can produce path length changes much larger than 1% and depending on the distribution of scattering particles and the elevation of the sun the changes can be either positive or negative. The OCO instrument under development at Jet Propulsion Laboratory (JPL) will measure the full spectrum of CO_2 and O_2 and the data are expected to provide enough information to permit a correction for the atmospheric scattering effects. Because we use a different technique the approach for our instrument is to employ the glint off water for the airborne measurements. Glint has two advantages – it is bright and therefore will dominate the weak scattering from aerosols and thin cirrus. Secondly the path length is known very precisely since the viewing angle to the glint can be measured and the location of the Sun can be calculated. Theoretical simulations show that our

instrument, employing the glint is capable of measuring the CO_2 column with a precision better than 0.3% for space or airborne platforms.

B. New sensor design

We are in a process of developing a reduced size and volume portable channel for CO_2 capable of doing simultaneous measurements with the AERONET (Aerosol Robotic Network) at NASA, Goddard. Fabry-Perot radiometer as a ground-based sensor has the potential to fill-in the sparse network of surface measurements – key in balancing the carbon budget. The instrument's low cost will enable its wide implementation in order to provide a broader range of intercomparison sites for the OCO instruments. For that purpose we designed a radiometer (Fig.7) which has a simpler configuration than the tested airborne instrument (Fig.1). The small radiometer consists of two sub-channels – the sub-channel that includes very narrow bandpass filter and the sub-channel, which detects the total light intensity limited by the wide bandpass filter spectral range. Laser scans of the two filters are shown on Fig.8. The CO_2 absorption lines from HITRAN database are also shown. The narrow filter is fitting into the gap of the P and R branches of the CO_2 absorption band near 1.57 micron. All other CO_2 absorption lines are blocked by the narrow filter this way. They are however detected by the wide filter making it the active channel for this sensor. Sensitivity of the ground-network version of the field instrument is expected to be comparable to that of the previous ground instrument. In Table 1 we summarized some of the instrument parameters.

C. Performance Simulations and Expected Results for Methane CH_4 and carbon isotope $^{13}CO_2$ sensors

A sensor for methane is under development. We modeled the expected performance of the instrument (Fig.9, top) as follows: First, we generated a synthetic spectrum for reflected light containing spectral features for CO_2, H_2O, and CH_4 from the HITRAN database [31]. Initially we assumed an average column mixing ratio of 1.8 ppm for methane. We calculated the solar flux signal received in the two subchannels (the FP and the Reference) for light that has passed through the atmosphere and been collected by the suntracker/telescope. After perturbing the total methane column by 1% we recalculate the signals. We compare the change in the ratio (FP/REF) caused by the perturbation to the detector noise of this ratio. The free parameters of the instrument design (eg. FP free spectral range, FP finesse, filter bandpass, filter edge slopes, instrument FOV) are varied in an effort to minimize response to changes in CO_2 and H_2O while maximizing response to CH_4. In the 1.6 micron region CH_4, CO_2, carbon monoxide (CO) and H_2O have significant absorption features. Our radiometer design is based on the attempt of increasing the signal for CH_4 and reducing that for others interfering species. It will have the capability of measuring CH_4 in both the Earth and Mars environment. For CH_4 measurements on Mars the thickness of the solid etalon is calculated to be 0.15 mm, the free spectral range (FSR) is 6.6 nm and the prefilter will be 11.4 nm wide. For the Earth measurements the solid etalon will have 0.359 mm thickness, FSR=2.6 nm and the prefilter will be 11.5 nm wide. On Earth only water vapor has significant abundance in the same spectral region. For a column average methane of 1.8 ppm and of 5000 ppm for water vapor this instrument has a theoretical signal to noise ratio of 1200:1 for methane and less than 1:1 for water in a one second averaging period. This means if the water vapor doubled from 5000 ppm to 10000 ppm it would only cause the instrument to make an error less than that arising from detector noise. Simulations for $^{13}CO_2$ and CO were done in the same way.

IV. CONCLUSION

We presented here a prototype passive Fabry-Perot based instrument for absorption measurements of total column carbon dioxide using sunlight at 1.58μm. This instrument has been demonstrated as a ground based sensor when used in conjunction with a positioning system to follow sun movement. Signals from these data trials were found to consistently track changes in air mass. Additionally, laboratory experiments and airborne measurements validate the instrument's sensitivity to changes in CO2. Additional water vapor channel was added to the system and prove to give reasonable results. New channels for carbon monoxide (CO), methane (CH4) and carbon isotope ($^{13}CO_2$) are under development. The theoretical simulations for them show that sufficient signal-to-noise ratios can be achieved.

The Fabry-Perot radiometer is a mature technology for ground based or airborne measurements capable of providing high precision and high spatial resolution data of carbon dioxide, oxygen, and water vapor. It is doing rapid measurements of the entire atmospheric column, has a relatively simple design and can use both nadir and glint viewing modes. The measurements can be used directly to validate products from a number of satellites currently operated by NASA and ESA. They can also be used as additional checks on the measurements of some of the lidar and *in situ* sensors.

ACKNOWLEDGMENT

This work was supported in part by the NASA Earth Sun-System Technology Office (ESTO), Instrument Incubator Program (IIP), grant NRA-01-OES-01 and NASA IRAD program. E. Georgieva thanks Brent Holben, Frederick S. Policelli, Jim Garvin and John Pearl for the valuable comments they kindly provided.

REFERENCES

[1] Francois-Marie Breon, "How do aerosols affect cloudiness and climate", *Science*, vol.313, pp.623-624, August, 2006.

[2] Y. J Kaufman and I. Koren, "Smoke and Pollution Aerosol Effect on Cloud Cover", *Science*, vol. 313, pp. 655-658, August, 2006.
[3] M.O. Andreae, C.D. Jones and P.M. Cox, "Strong present-day aerosol cooling implies a hot future", *Nature*, vol. 435, pp.1187-1190, June 2005.
[4] T.L. Anderson et al, "An "A-Train" Strategy for Quantifying Direct Climate Forcing by Anthropogenic Aerosols", *American Meteorological Society*, Vol. 86, No 12, pp.1795-1809, December, 2005.
[5] A. S. Ackerman, O.B. Toon, D.E. Stevens, A.J. Heymsfeld, V. Ramanathan, E.J. Welton," Reduction of Tropical Cloudiness by Soot", *Science*, vol.288, pp.1042-1047, May, 2000.
[6] P.J. Crutzen, "Geology of mankind", *Nature*, vol. 415, pp.23-23, January, 2002.
[7] J.L. Sarmiento, N. Gruber, "Sinks for Anthropogenic Carbon", *Physics Today*, vol.55, No 8, pp. 30-36, August, 2002.
[8] Climate Change 2007 – The Physical Science basis, Intergovernmental Panel on Climate Change, Cambridge, ISBN-13:9780521705967. (http://ipcc-wg1.ucar.edu/wg1/wg1-report.html.
[9] Beer Reinhard, "TES on the Aura Mission: Scientific Objectives, Measurements, and Analysis Overview", *IEEE Transactions on Geoscience and Remote Sensing*, vol.44, No.5, pp.1102-1105. May, 2006.
[10] E. Dufour, and F. Breon,: "Spaceborne estimate of atmospheric CO2 column by use of the differential absorption method: error analysis.", *Applied Optics* vol.42, No18, pp.3595-3609, June, 2003.
[11] P.J. Rayner, and D.M. O'Brien, "The utility of remotely sensed CO_2 concentration data in surface source inversions", *Geophys.Res. Letters*, vol.28, No.1, pp.175-178, January, 2001.
[12] D.M. O'Brien, P.J. Rayner, "Global observations of the carbon budget 2. CO_2 column from differential absorption of reflected sunlight in the 1.61 mm band of CO2", *Journal of Geophysical Research*, vol. 107 (D18), Art.No 4354, pp.1-16, September , 2002.
[13] U.S. Global Carbon Cycle Science Program 2007, Highlights of Recent Research and Plans for FY, Chapter 5, pp.114-120, 2007.
[14] C.M. Cooney, "Uncertainties linked to water vapor's role in climate changes", *Environmental Science &Technology*, vol.33, No.23, pp. 489A-489A, 1999.
[15] V. Wulfmeyer & C. Walther, "Future performance of ground-based and airborne water-vapor differential absorption lidar, Parts I and II", *Applied Optics*, vol.40, pp.5304-5336, 2001.
[16] J Acarreta and P. Stammes, "Calibration Comparison Between SCIAMACHY and MERIS Onboard ENVISAT", *IEEE Geoscience and Remote Sensing Letters*, vol.2, No.1, pp.31-35, January, 2005.
[17] GLOBALVIEW-CO_2, Cooperative Atmospheric Data Integration Project - Carbon Dioxide, NOAA CMDL, Boulder, Colorado.
[18] K.R. Gurney, Y.H. Chen, T. Maki, S.R. Kawa, A. Andrews, Z.X. Zhu, "Sensitivity of atmospheric CO_2 inversions to seasonal and interannual variations in fossil fuel emissions", *J.Geophys. Res.*, vol. 110, D10308, pp.1-13, May, 2005.
[19] E.M. Georgieva, E. Wilson, M. Miodek, W. Heaps , "Total Column Oxygen Detection Using Fabry-Perot Interferometer", *Optical Engineering*, vol. 45 (11), Paper No115001, pp.1-11, November, 2006.
[20] W. Heaps, S.R. Kawa, E. Georgieva, et al, "Ultra-precise measurement of CO_2 from space", Conference on Passive Optical Remote Sensing of the Atmosphere and Clouds IV, *Passive Optical Remote Sensing of the Atmosphere and Clouds*, pp. 136-145 , November, 2004.
[21] E.L. Wilson, E. M. Georgieva, W. S. Heaps, "Development of a Fabry-Perot interferometer for ultra-precise measurements of column CO_2", *Measurement Science and Technology*, Vol. 18, pp. 1495-1502, March, 2007.
[22] E. M. Georgieva, et al., "Precise measurement of CO_2 from space using Fabry-Perot based optical setup: current status and development", *Proc SPIE Earth Observing Systems XI*, vol.6296, pp.62961G-62961G-12, 2006.
[23] E. M. Georgieva et al. "Atmospheric column CO_2 and O_2 absorption based on Fabry-Perot etalon for remote sensing", *Proc. SPIE Earth Observing Systems X*, vol.5882, pp.58820G-1-58820G-9. 2005.
[24] D. Crisp, C Johnson, "The orbiting carbon observatory mission", *Acta Astronautica*, vol. 56, No1-2, pp.193-197, 2005.
[25] D. Crisp et al., " The orbiting carbon observatory (OCO) mission", *Advances in Space Research*, vol. 34 , No 4, pp.700-709, 2004.
[26] D. Crisp et al., "The NASA Orbiting Carbon Observatory: Measuring the column-averaged Atmospheric CO_2 mole fraction from space", *SPIE, Sensors, Systems, and next-generation Satellites X*, pp.U119-U128, 2006.
[27] R. Haring et al., "The orbiting carbon observatory (OCO) instrument optical design", *SPIE, Current Developments in Lens Design and Optical Engineering V*, pp. 51-62, 2004.
[28] J. Vaughan, "The Fabry-Perot Interferometer: history, theory, practice, and applications", Bristol, England, 1989.
[29] G. Hernandez, "Fabry-Perot interferometers", Cambridge, New York, 1986.
[30] B. Bolin, "The carbon cycle", *Sci. Amer.*, vol. 223(3), pp. 124-132, 1970.
[31] L.S. Rothman et al, 'The HITRAN 2004 molecular spectroscopic database ',Journal of Quantitative Spectroscopy &Radiative Transfer, vol.96, pp.139–204, 2005.

Elena Georgieva received her M.S. in physics from Sofia University, Sofia, Bulgaria, She received her PhD in physics in 1998 from the University of Sofia. She was a research associate at Lasers and Optical characterization Laboratory, Georgetown University where she worked on nanoparticles characterization and correlation spectroscopy. She also was a research associate at NIST Center for neutron research and Johns Hopkins University. For four years she was a Senior Systems Scientist/Engineer at Science systems and Applications and worked at Goddard Laser and Electro-optics branch on instrument development for measurement of atmospheric species. She has research experience in remote sensing, data analysis and validation, instrument development, spectroscopy, interferometry, 3-D imaging laser radar system and polarimetry. She is currently an Associate Research Scientist with Goddard Earth Sciences and Technology Center (GEST), University of Maryland Baltimore county UMBC & NASA Goddard Space Flight Center. She is a member of Optical Society of America and The International Society for Optical Engineering (SPIE).

Wm. S. Heaps has a long and distinguished career in atmospheric science and remote sensing technology. With a B.A. in Physics from Rice University and a Ph.D. from University of Wisconsin he joined Goddard in 1977 after a brief stint as an NRC postdoc. His first effort was development of a balloon borne laser induced fluorescence instrument that succeeded in making some of the first measurements of stratospheric hydroxyl radical.
In the late 1980's he served on the mission planning group for the UARS satellite. At the same time he developed an airborne Raman lidar system to measure water vapor and methane and aided in the development of the Solar Disk Sextant that made the most precise ever measurements of the diameter and shape of the Sun.
In 1998, he left the Atmospheric Chemistry and Dynamics Branch to become Branch Head of the Laser & Electro-Optics Branch. While serving as Branch Head he became the Goddard PI for NASA's Laser Risk Reduction Program administering more than 20M$ over 5 years in a program to enhance performance and reliability of lasers for space borne remote sensing.
During this period he also wrote a successful proposal to the Earth Science Technology Office's Instrument Incubator Program to begin the development of the Fabry-Perot interferometer and a successful proposal to the newly formed Office of Exploration for 3D Laser Robot Vision. He has participated in more than 15 balloon launches. He has served as an airborne experimenter in a number of international measurement campaigns including TOTE/VOTE, SOLVE I, SOLVE II, PAVE and INTEX-B operating lidars as well as the Fabry-Perot Interferometers.
Today he serves on the staff of the Instrument Systems and Technology Division as Senior Staff Engineer for Lasers and Electro-Optics.

E. Wilson has research experience in physical chemistry, spectroscopy, and combustion and specializes in instrument development for measurement of atmospheric species. Dr. Wilson joined the Laser and Electro-Optics Branch as a physicist in 2005 following a NRC Postdoc at this branch from 2002-2005. Her education includes a Ph.D. in physical chemistry from The George Washington University in Washington, DC (2002), a M.A. in chemistry from Boston University (1999), and a B.S. in

chemistry in chemistry from The University of Montana in Missoula, MT (1995). She was the recipient of the American Institute of Chemists Outstanding Chemistry Student Award (1995).

Previous positions held by Dr. Wilson include Graduate Research Assistant at The George Washington University conducting spectroscopic measurement of trace gases in laboratory scale methane flames (1999-2002), Science Education Assistant at the Lemelson Center for Invention and Innovation at the National Museum of American History, Smithsonian Institution producing science education programs for middle school students (1997-1999), and Graduate Research Fellow at Boston University studying collisional energy transfer reactions (1995-1997).

TABLE 1
INSTRUMENT PARAMETERS

The optical aperture for the airborne FP radiometer (Fig.1) is 0.051 m. For the small version FP (Fig.8) the size is reduced to 0.025m. The FOV is 0.086 deg for both instruments. The dimensions of the airborne FP radiometer are 0.72 x 0.35 x 0.35m and the dimensions for the small FP radiometer are 0.27 x 0.2 x 0.09 m.

	Bandpass filters	FSR of the FP etalons	Resolution $\Delta\lambda/\lambda$	Sensitivity
Channels	FLIGHT VERSION of the FP RADIOMETER			
Carbon dioxide (CO_2)	1567-1574nm	0.306 nm	13898	2.3ppm in 1 sec (direct light),2% reflected light
Oxygen (O_2) pressure	760-764 nm	2.212 nm	2422	0.88 mbar
Oxygen (O_2) temperature	767-771nm	0.575 nm	4366	0.4 deg
	SMALL VERSION of the FP RADIOMETER			
Water vapor (H_2O)	917.7-1101nm & 925-970nm	Bandpass filter, holographic notch filter		2% for 1 sec
Carbon dioxide (CO_2)	1568-1584nm 1573.5-1578 nm	Bandpass filters		Under test
Methane (CH_4)	1634-1644nm	2.6 nm	6559	Under test
Carbon isotope ($^{13}CO_2$)	2111-2121nm	0.4227 nm	42000	Under test

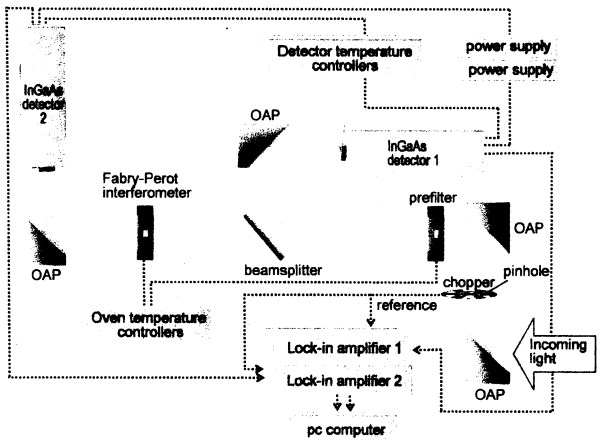

Fig. 1. Optical and electronic schematic for the CO_2 channel of the Fabry-Perot instrument. Incoming light is collimated by two off axis parabolic gold mirrors (OAP's). The light is divided into Fabry–Perot (detector 2) and reference (detector 1) sub-channels, measuring changes in CO_2 absorption and solar flux, respectively. The ratio of these signals can then be related to changes in the CO_2 column.

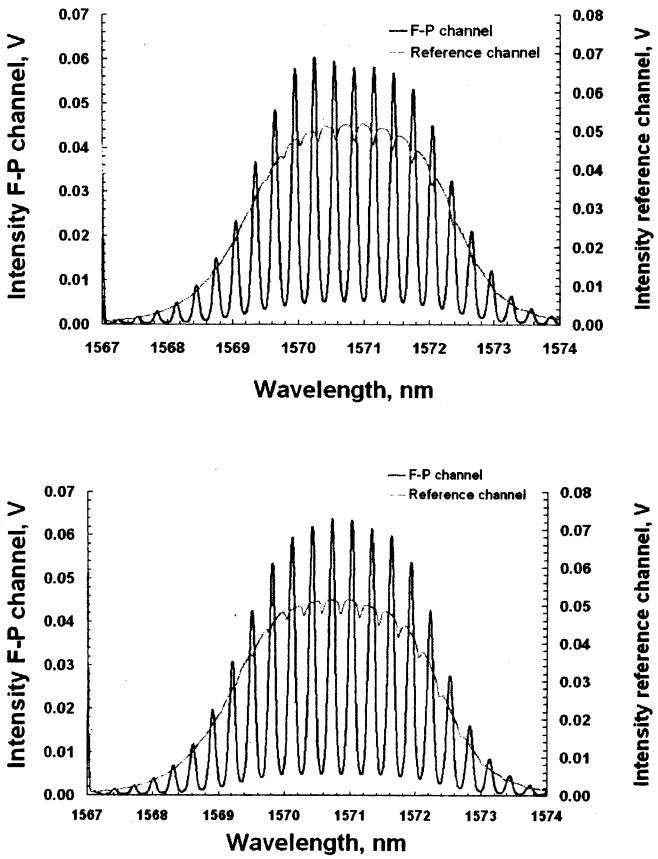

Fig. 2. Alignment of etalon transmission bands (blue) with CO_2 absorption lines (pink) can be adjusted by changing the etalon temperature. An etalon temperature of 54°C (top) shows better alignment than at 42°C (bottom).

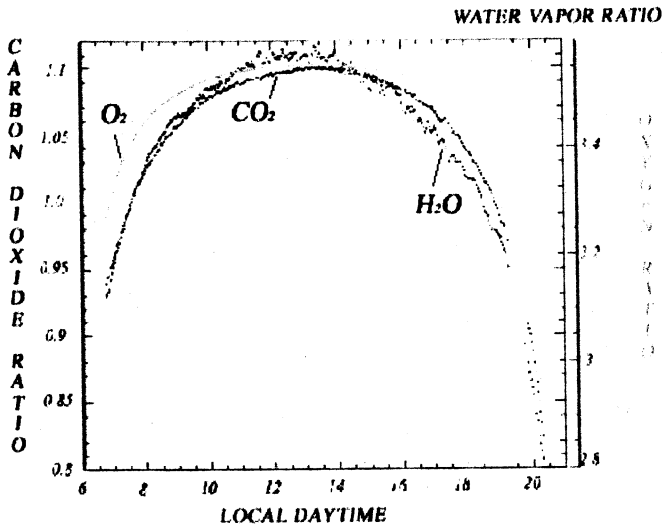

Fig. 3. The FP (Fabry-Perot) to Reference channel ratio is plotted as a function of local time for an O_2 instrument (yellow), a CO_2 instrument (blue), and a water vapor instrument (red).The principal variation is that arising from the change in air mass as the sun rises and sets throughout the day. Mesurement is done June 30, 2006, data were collected every 0.1 sec and averaged for every 120seconds.

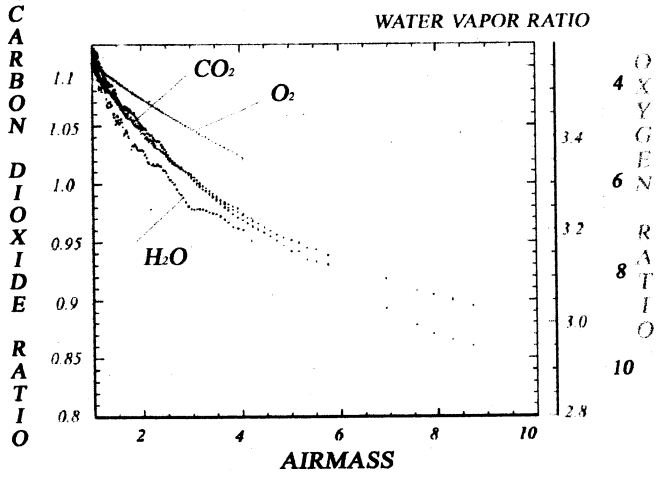

Fig. 4. Here the ratios from the previous figure are plotted against the calculated air mass. The AM and PM values for O_2 are virtually the same and cannot be distinguished. The CO_2 channel shows some slight variation throughout the day probably arising from consumption by plants. The water vapor channel shows considerable variation consistent with typical changes in humidity throughout a day.

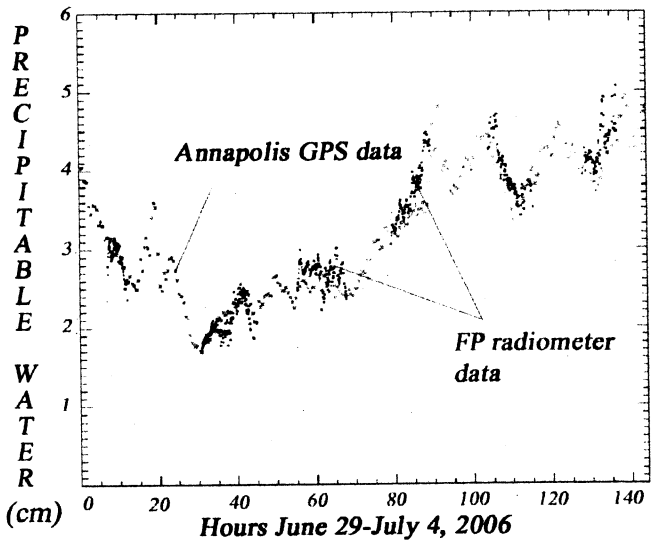

Fig. 5. Water vapor data taken June 29, 2006 at Goddard using FPICC (blue dots) compared to Annapolis water vapor data (red dots). The FPICC data and the NOAA data using GPS technology show remarkable agreement.

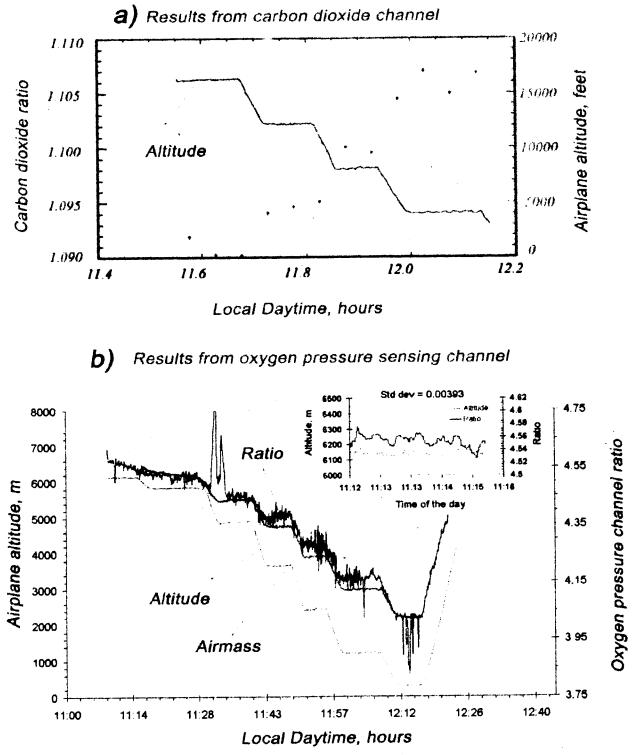

Fig. 6. The instruments response to the altitude in meters at airborne mission.a) The CO_2 ratio of Fabry-Perot to Reference signals is shown compared to changes in altitude on a May 14, 2004 flight. As the aircraft descends the photon pathlength gets shorter so the absorption in the Fabry-Perot subchannel decreases. b) The Ratio for the pressure-sensing channel (O_2) and air mass as a function of time are shown. The embedded graph shows the blown images of the measured Ratio and altitude for four minutes. The standard deviation is calculated to be 0.00393.

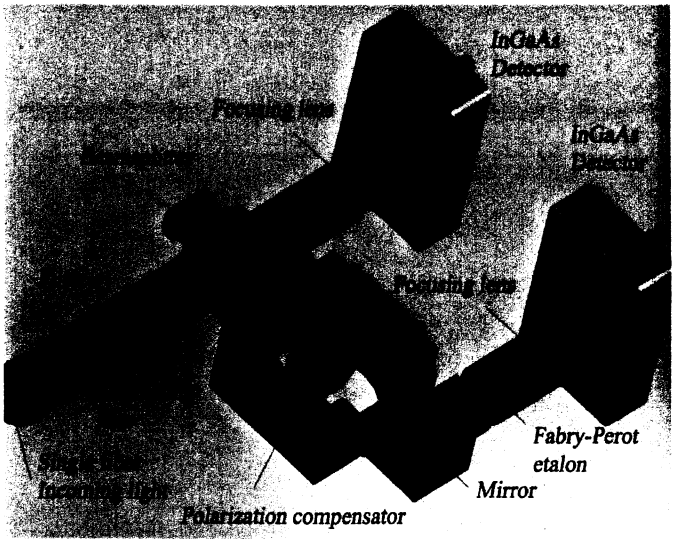

Fig. 7. A representation of the physical design of the small-size CO_2 instrument.

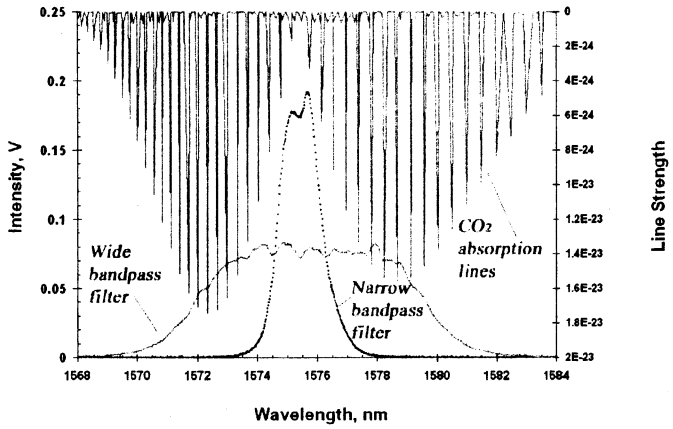

Fig. 8. Laser scan of the two filters for the small CO_2 radiometer. The CO2 absorption lines from HITRAN database are also shown. The narrow band versus wide band sub-channels ratio will be sensitive to CO_2 changes in the atmosphere.

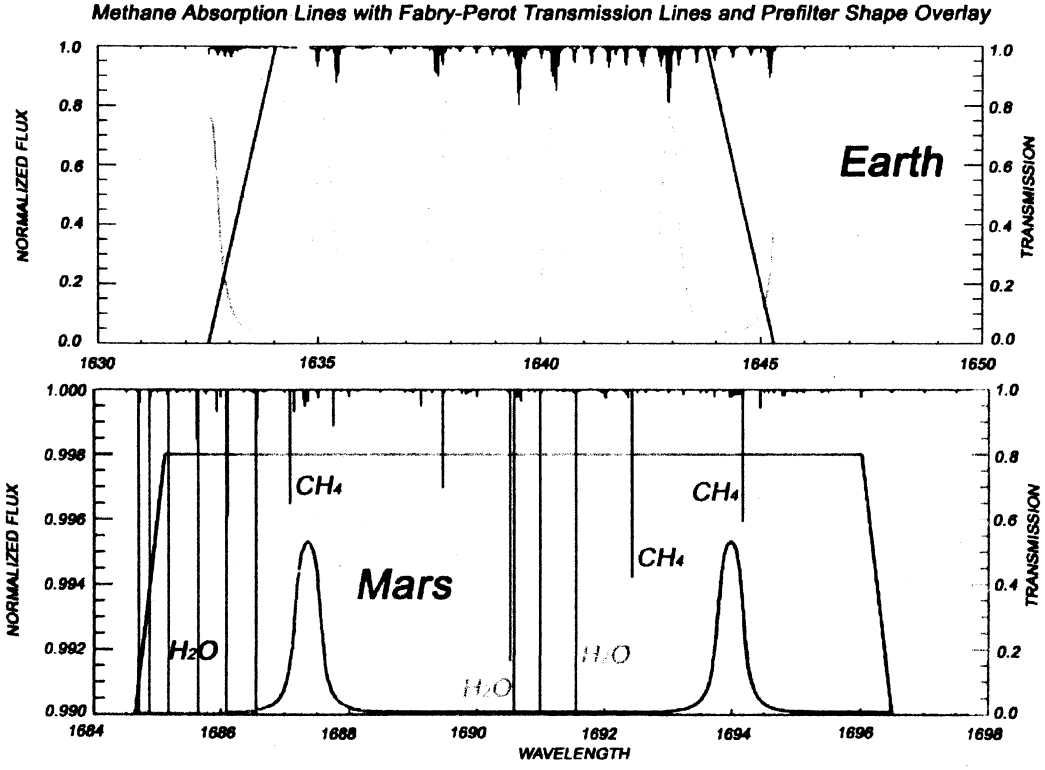

Fig. 9. The transmission bands of the solid Fabry-Perot etalons (yellow and green) and pass bands of the narrow prefilters (red) are shown. The top picture is representing the model simulations for the Earth atmosphere and the bottom picture – for the Mars atmosphere. The Martian atmosphere is less than 1% as dense as Earths. The absorption features of CH_4 are correspondingly weaker. Fabry-Perot transmission bands are shown aligned with some CH_4 lines. There is also a strong absorption from water vapor (H_2O) which can be cancelled by positioning of the etalon and the prefilter.